Robust Design of Body Slip Angle Observer with Cornering Power Identification at Each Tire for Vehicle Motion Stabilization

Yoshifumi Aoki, Zhao Li, Yoichi Hori

Department of Electrical Engineering
The University of Tokyo
7-3-1, Hongo, Bunkyo-ku, Tokyo 113-8656,Japan
y-aoki@horilab.iis.u-tokyo.ac.jp
http://mizugaki.iis.u-tokyo.ac.jp/

***Abstract*— Body slip angle is important for vehicle's safety. However as sensors to measure β are very expensive, we need to estimate β from only variables to be measurable.**

In this paper,we propose a novel method based on γ and side acceleration a_y. To make this observer more robust, we design the observer's gain matrix for robustness and propose how to identify cornering power at each tire.

Next, we proposed new control methods for 2-Dimension control. We control β by yaw moment with PID controller. This method is known as DYC (Direct Yaw momnet Control) in Internal Combustion engine Vehicles (ICVs). However, the torque difference can be generated directly with in-wheel motors.

We performed experiments by UOT MarchII. The experimental results proved that our proposed method was good.

Fig. 1. UOT MarchII

I. Introduction

Electric Vehicles (EVs) are environment-friendly and expected to be a promising solution for solving today's energy problems. Thanks to the dramatic improvement of motors' and batteries' performances, EVs will become more popular in the near future. It is predicted that before pure EVs, Hybrid EVs (HEVs) will be widely used in the next 10 years.

However, it is not well recognized that EVs have other advantages over Internal Combustion engine Vehicles (ICVs) [1]. Those advantages can be summarized in three aspects.

First, motor's torque generation is fast and accurate. Electric motor's torque response is only several milliseconds, which is 10-100 times as fast as combustion engine's. This advantage can enable us to realize high performance control of EVs.

Second, motor torque can be known precisely. Therefore we can easily estimate driving and braking forces between tire and road surface in real-time. This advantage can be used to realize novel control based on road condition.

Third, in-wheel motors can be installed in EVs' each rear and front tires. We can control each torques of the four motors so that it is easier to control EVs' slip angle β and yaw rate γ than ICVs'. In order to make full use of EVs' advantages, it is essentially important to research on β and γ control and β observer.

In order to estimate β, we utilize full order linear observer because nonlinear observer is too complex to control β and γ. We design observer's gain matrix and propose a new method based on γ and side acceleration a_y. Additionally to make the novel observer more robust against cornering power CP, we proposed a novel method of cornering power identification.

We did experiments by using UOT March II. Experiments show the proposed observer can estimate β accurately and the observer is robust against parameter variation.

Next, we design controller to control only β. If β is too big, EVs cannot be controlled and spin off. β should be controlled. We utilize Model Following Control (MFC) and PID controller. Experiments by UOT March II demonstrated the effectiveness of our control method.

II. Modeling of EVs

We use two-wheel model [2] for two-dimensional movement of EVs as shown in Fig. 2. Generally, in order to describe vehicle's two dimension movement exactly, four-wheel model is needed. However because four wheeled model is non-linear model, it cannot be used for linear observer design. Where P is the center of gravity, l_f is the distance from P to the front wheel, l_r is the distance from P to the rear wheel, α_f is the front wheel slip angle, α_r is the rear wheel slip angle and δ_f is actual steering angle at tire.

Usually, we express state equations with β, γ, and vehicle speed v. Motion equations are expressed in Equs. (1).

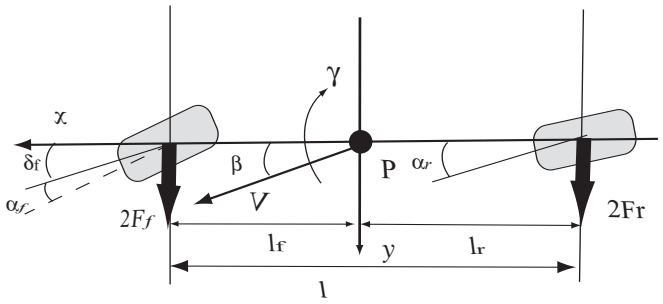

Fig. 2. Two-wheel model of vehicle motion

From Equs. (1) we can get the state equation:

$$\dot{x} = \boldsymbol{A}\boldsymbol{x} + \boldsymbol{B}\boldsymbol{u} \tag{1}$$

$$\boldsymbol{A} = \begin{bmatrix} \frac{-(C_{fl}+C_{fr}+C_{rr}+C_{rl})}{mv} & \frac{-l_f(C_{fl}+C_{fr})+l_r(C_{rl}+C_{rr})}{mv^2}-1 \\ \frac{-(l_f(C_{fl}+C_{fr})+l_r(C_{rl}+C_{rr})}{I} & \frac{-l_f^2(C_{fl}+C_{fr})-l_r^2(C_{rl}+C_{rr})}{Iv} \end{bmatrix}$$

$$\boldsymbol{B} = \begin{bmatrix} \frac{C_{fl}+C_{fr}}{mv} & 0 \\ \frac{l_f(C_{fl}+C_{fr})}{I} & \frac{1}{I} \end{bmatrix}, \quad \boldsymbol{x} = \begin{bmatrix} \beta \\ \gamma \end{bmatrix}, \quad \boldsymbol{u} = \begin{bmatrix} \delta_f \\ N \end{bmatrix}$$

$C_{fl} \sim C_{rr}$ are cornering powers at each tire, which is defined as Equs. (2) and (3).

$$C_f = \frac{\partial F_f}{\partial \alpha_f} \mid_{\alpha_f=0} \tag{2}$$

$$C_r = \frac{\partial F_r}{\partial \alpha_r} \mid_{\alpha_r=0} \tag{3}$$

Input N is yaw-moment by driving force distribution, which is expressed by Equs. (4).

$$N = \frac{d}{2}(-F_{x\_fl} + F_{x\_fr} - F_{x\_rl} + F_{x\_rr}) \tag{4}$$

Because N cannot be measured, we must estimate N.

A. yaw moment estimation

To estimate N, It is necessary to estimate driving forces F_d. We proposed this yaw-moment estimation method, which is defined as Equs. (6) and expressed by Fig. (5).

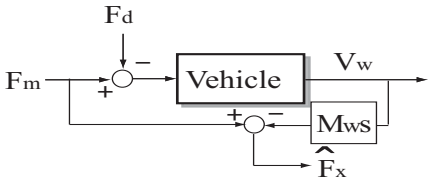

Fig. 3. driving force estimator

$$\hat{F}_x = F_m - M_w \frac{dV_w}{dt} \tag{5}$$

$$\hat{N} = \frac{d}{2}(-\hat{F}_{x\_fl} + \hat{F}_{x\_fr} - \hat{F}_{x\_rl} + \hat{F}_{x\_rr}) \tag{6}$$

III. Design of proposed linear observer

A. Restructuring of output equation by using side acceleration a_y

Various methods for estimating β were proposed previously. For example, direct integral method [3] estimates β based on Equ. (7). In this method, estimated β contains steady state error, therefore it can't estimate β exactly. Nonlinear observers [4] [5] [6] [7] aim to design an accurate model based on actual vehicle's dynamics and to estimate β. These methods are suitable for simulation. But due to the complexity of the models, these methods are difficult for β estimation in real-time.

$$v(\dot{\beta} + \gamma) = a_y \Leftrightarrow \beta = \int (\frac{a_y}{v} - \gamma) dt \tag{7}$$

The advantage of conventional linear observers is it's simple structure. However they are not robust enough against model error. Moreover it cannot estimate β exactly in non-linear region.

In order to overcome these disadvantages, we propose a novel linear observer in this paper. Unlike conventional observers using only γ as measurable signal, we utilize a_y together with γ to construct the linear observer [8], which can estimate β in non-linear region.

To design the observer, it is necessary to restructure output equation by measurable parameters. Using Equs. (1) and (7), a_y can be restructured as:

$$a_y = v(a_{11}\beta + a_{12}\gamma + b_1\delta + \gamma) \tag{8}$$

The output equation is:

$$\boldsymbol{y} = \boldsymbol{C}\boldsymbol{x} + \boldsymbol{D}\boldsymbol{u} \tag{9}$$

$$\boldsymbol{C} = \begin{bmatrix} 0 & 1 \\ va_{11} & v(a_{12}+1) \end{bmatrix}, \quad \boldsymbol{D} = \begin{bmatrix} 0 & 0 \\ vb_{11} & 0 \end{bmatrix}, \quad \boldsymbol{y} = \begin{bmatrix} \gamma \\ a_y \end{bmatrix}$$

B. Full order linear observer

We use full order observer, which is defined by the following equations.

$$\dot{\hat{\boldsymbol{x}}} = \boldsymbol{A}\hat{\boldsymbol{x}} + \boldsymbol{B}\boldsymbol{u} - \boldsymbol{K}(\hat{\boldsymbol{y}} - \boldsymbol{y}) \tag{10}$$

$$\hat{\boldsymbol{y}} = \boldsymbol{C}\hat{\boldsymbol{x}} + \boldsymbol{D}\boldsymbol{u} \tag{11}$$

where K is observer matrix gain. $\hat{x}$ s estimated x. The estimation error equation $e = \hat{\beta} - \beta$ should satisfy the following error equation:

$$\dot{e} = (A - KC)e \tag{12}$$

Full order observer's characteristic is decided by value of matrix gain K.

C. Design of gain matrix for robustness

If the selected matrix gain is inadequate, the linear observer will have a poor robust performance against model error and sometimes cannot estimate β exactly. To decide matrix gain, we must consider two important factors. First, the observer must be designed robust against model error. Since two-wheel model is used in our design, some model error exists more or less. Especially, cornering power Cf and Cr depend on road condition and loads on each tires. Therefore, their values are changing and cannot be measured. Second, all eigenvalues of $A - KC$ must be located in stable region. $A - KC$ is the state transition matrix of Equ. (11). The positions of $A-KC$ eigenvalues will affect control system's time response

performances, such as overshoot, rising time and settling time. To make the observer robust, we referred [9]. By calculate Equs. (7) and (8), we can get $\hat{\beta}$:

$$\dot{\hat{\beta}} = a_{11}\hat{\beta} + a_{12}\hat{\gamma} + b_{11}\delta_f - k_{11}(\hat{\gamma} - \gamma) - k_{12}(\hat{a_y} - a_y) \quad (13)$$

State equation of β is expressed as:

$$\dot{\beta} = a_{11}'\beta + a_{12}'\gamma + b_{11}'\delta_f \quad (14)$$

a_{11}', a_{12}' and b_{11}' are the real values. Any model error is not contained in this equation.

By Equs. (13) and (14), the state equation for $\hat{\beta} - \beta$ is given by following equation.

$$\begin{aligned}\dot{\hat{\beta}} - \dot{\beta} = {} & a_{11}(1 - k_{12}v)(\hat{\beta} - \beta) \\ & + [a_{12} - k_{12}v(a_{12} + 1) - k_{11}](\hat{\gamma} - \gamma) \\ & - (1 - k_{12}v)(a_{11}' - a_{11})\beta \\ & - (1 - k_{12}v)(a_{12}' - a_{12})\gamma \\ & - (1 - k_{12}v)(b_{11}' - b_{11})\delta_f \end{aligned} \quad (15)$$

The best condition for robustness in Equ. (15) is:

$$1 - k_{12}v = 0 \Leftrightarrow k_{12} = \frac{1}{v} \quad (16)$$

Based on consideration of pole assignment and robustness against cornering power, K is decided as:

$$K = \begin{bmatrix} \frac{l_f(C_{fr}+C_{fl}) - l_r(C_{rr}+C_{rl})}{(C_{fr}+C_{fl})(C_{rr}+C_{rl})(l_f - l_r)^2}\lambda_1\lambda_2 I - 1 & \frac{1}{v} \\ -\lambda_1 - \lambda_2 & \frac{m((C_{fr}+C_{fl})l_f^2 + (C_{rr}+C_{rl})l_r^2)}{(C_{fr}+C_{fl})l_f - (C_{rr}+C_{rl})l_r)I} \end{bmatrix}$$

λ_1 and λ_2 are the assigned poles of the observer.

Fig. 4 is simulation result of the designed observer. This result shows us that the novel proposed observer can estimate β well.

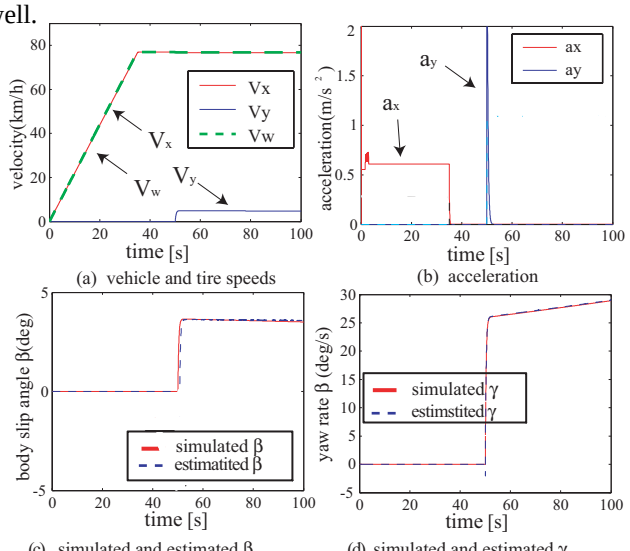

(a) vehicle and tire speeds (b) acceleration

(c) simulated and estimated β (d) simulated and estimated γ

Fig. 4. Simulation result

IV. Proposed Method of Cornering Power Identification

A. lateral force estimator for friction circle estmation and cornering power identification

By driving force estimator shown as Equ. 5, we can know longitudinal forces at tire. If lateral force can be estimated, we can know friction circle of tire. Lateral force is needed to estimate.

Additionally, cornering power CP can be identified from estimated side forces by using Equ. 17 and fixed trace method.

$$F_y = C_f\alpha \quad (17)$$

Lateral forces are estimated by Equs.19, which is derived from linear equation of vehicle motion shown as Equ. 18.

$$\begin{aligned} I\dot{\gamma} &= 2F_{yf}l_f cos\delta_f - 2F_{yr}l_r + N \\ ma_y &= 2F_{yf}\cos\delta_f + 2F_{yr} \end{aligned} \quad (18)$$

$$\Updownarrow$$

$$\begin{aligned} \hat{F}_{yf} &= \frac{I\dot{\gamma} + ml_r a_y - N}{2(l_f + l_r\cos\delta_f)} \\ \hat{F}_{yr} &= \frac{-I\dot{\gamma} + ma_y l_f + Ncos\delta_f}{2(l_r\cos\delta_f + l_f)} \end{aligned} \quad (19)$$

Moreover, we proposed the method of lateral force estimation at each tire from Equs. 19 and 20.

Lateral force F_y is also defined by Equ. 20.

$$F_y = \mu(\lambda_y)F_z \quad (20)$$

where F_{z_f} and F_{z_r} which are defined by Equ. 21, are average normal components of reaction at front and rear tires. $\mu(\lambda_y)$ is friction coefficient of lateral direction.

$$\begin{aligned} F_{z\_f} &= \frac{m(l_r g - ha_x)}{2(l_f + l_r)} \\ F_{z\_r} &= \frac{m(l_r g + ha_x)}{2(l_f + l_r)} \end{aligned} \quad (21)$$

Equ. 20 shows us that lateral force be proportional to the product of μ_y and normal component of reaction. Left and right tires' μ are nearly equal. So lateral force is directly proportional to F_z. F_z can be calculated by Equ. 22.

$$\begin{aligned} F_{z\_fr} &= \frac{m(l_r g - ha_x)}{2(l_f + l_r)} + \frac{hma_y}{d} \\ F_{z\_fl} &= \frac{m(l_r g - ha_x)}{2(l_f + l_r)} - \frac{hma_y}{d} \\ F_{z\_rr} &= \frac{m(l_r g + ha_x)}{2(l_f + l_r)} + \frac{hma_y}{d} \\ F_{z\_rl} &= \frac{m(l_r g + ha_x)}{2(l_f + l_r)} - \frac{hma_y}{d} \end{aligned} \quad (22)$$

where h is the distance from P to the ground, a_y is lateral acceleration and a_x is longitudinal acceleration.

From Equs. 20 $\sim$ 22, we can get lateral forces at each tire.

$$\begin{aligned} \hat{F}_{y\_fr} &= \mu(\lambda_{y\_f})F_{z\_fr} = \mu(\lambda_{y\_f})F_{z\_f}\frac{F_{z\_fr}}{F_{z\_f}} \\ &= \hat{F}_{yf}(1 + \frac{2(l_f + l_r)ha_y}{d(l_r g - ha_x)}) \\ \hat{F}_{y\_fl} &= \mu(\lambda_{y\_f})F_{z\_fr} = \mu(\lambda_{y\_f})F_{z\_f}\frac{F_{z\_fr}}{F_{z\_f}} \\ &= \hat{F}_{yf}(1 - \frac{2(l_f + l_r)ha_y}{d(l_r g - ha_x)}) \\ \hat{F}_{y\_rr} &= \mu(\lambda_{y\_f})F_{z\_fr} = \mu(\lambda_{y\_f})F_{z\_f}\frac{F_{z\_fr}}{F_{z\_f}} \end{aligned} \quad (23)$$

$$= \hat{F}_{yr}(1 + \frac{2(l_f + l_r)ha_y}{d(l_r g + ha_x)})$$

$$\hat{F}_{y\_rl} = \mu(\lambda_{y\_f})F_{z\_fr} = \mu(\lambda_{y\_f})F_{z\_f}\frac{F_{z\_fr}}{F_{z\_f}}$$

$$= \hat{F}_{yr}(1 - \frac{2(l_f + l_r)ha_y}{d(l_r g + ha_x)})$$

Fig. 5 is simulation result. This result shows that the poposed lateral force estimator can estimate lateral forces at each tire.

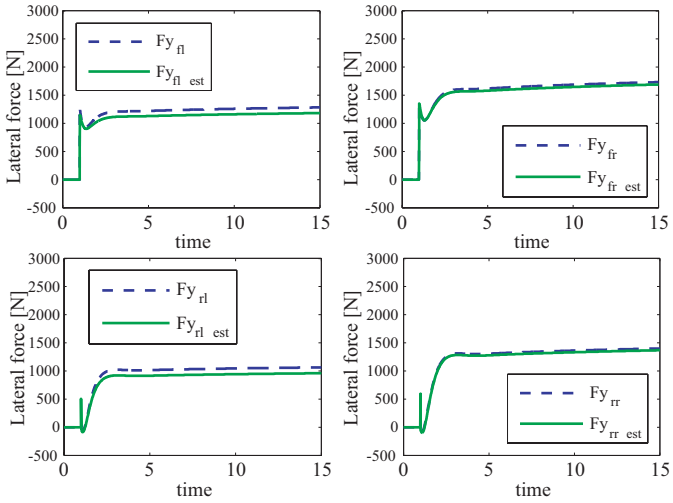

Fig. 5. Simulation result;lateral force estimation

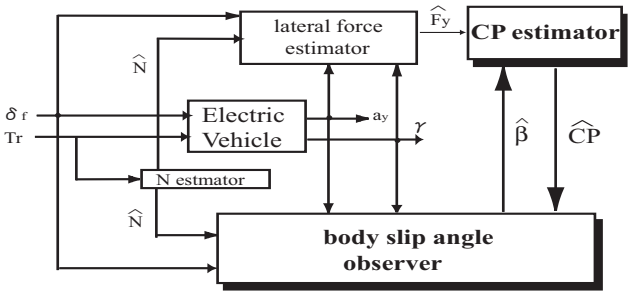

Fig. 6. conrnering power estimator

TABLE I
SENSORS OF UOT MARCH*II*

PC to control	Pentium MMX 223[MHz]
	AMD K6-233[MHz]
OS	Slackware Linux 3.5
	RTLinux rel. 9K
encoder pulse number	3600[ppr]
acceleration sensor	ANALOG DEVICES ADXL202
Yaw rate sensor	HITACHI OPTICAL FIBER GYROSCOPE HOFG-CLI(A)
Noncontact Optical sensor	CORREVIT S-400

V. CORNERING POWER IDENTIFICATION

As shown in the preceding chapter, lateral force can be estimated by the proposed method. We apply Equ. 17 to adaptive identification (Equ. 24).

$$\begin{aligned} y[k] &= \varphi^T[k]\hat{\theta}[k] + e[k] \\ \hat{\theta}[k] &= \hat{\theta}[k-1] + \frac{P[k-1]\varphi[k](y[k] - \varphi^T[k]\hat{\theta}[k-1])}{\kappa_2 + \varphi^T[k]P[k-1]\varphi[k]} \\ P[k] &= \frac{1}{\kappa_1}(P[k-1] - \frac{P[k-1]\varphi[k]\varphi^T[k]P[k-1]}{\kappa_2 + \varphi^T[k]P[k-1]\varphi[k]}) \end{aligned} \quad (24)$$

We utilize fixed trace method. κ_1 and κ_2 are expressed as:

$$\kappa_1 = \kappa, \quad \kappa_2 = 1 \quad (25)$$

$$\kappa = 1 - \frac{\|P[k-1]\varphi[k]\|^2}{1 + \varphi^T P[k-1]\varphi[k]}\frac{1}{\xi} \quad (26)$$

where ξ is trace gain defined by following equation in case of fixed trace method:

$$\xi = trP[k] = const. \quad (27)$$

In this case, y is lateral foce, φ is tire slip angle α and θ is cornering power.

VI. STRUCTURE OF ESTIMATING BODY SLIP ANGLE

We estimate body slip angle β by the proposed observer based on γ and a_y with cornering power identification. This system is shown in Fig. 6.

In this system, body slip angle β and cornering power estimate each other.

VII. EXPERIMENTAL DEMONSTRATION FOR OBSERVER BY UOT MARCH *II*

A. Experiment setup for the proposed observer

UOT March*II* is our experimental EV built to prove EVs' advantages. We made this EV by ourselves, which is remodeling of Nissan March. The EV equips acceleration sensor, gyro sensor and noncontact speed meter which enable us to measure β. Table. I explains specification.

We did various experiments and some experimental results were shown you. Vehicle velocity, driver's input steering wheel angle δ and road type were changed to test the effectiveness and robustness of the proposed observer and controller. While the experiment was done, road type was changed from dry road to wet road. But observer's and controller's parameters are kept unchanged. Steering angle was changed freely by the test driver.

We recorded β, γ, δ, v, V_w, F_m and a_y in hard disk drive by the sampling time of 1 [ms] and calculated by Matlab.

B. Experimental results for the proposed observer

Figs. 7 and 8 show two experiments' results under the difference conditions.

Fig. 7 shows experimental results in linear region. Fig. 7 (a) is measured and estimated β. Fig. 7 (b) is identified cornering power. Fig. 7 (c) and (d) are measured and output a_y and γ.

In Fig. 7 (a), EV is in linear region because steering angle δ is small. Fig. 7 shows us that the novel proposed observer can estimate β well in linear region. Even if we cannot know cornering power, we can know precise β by cornering power identification.

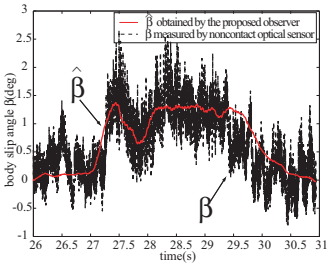

(a)measured value and estimation of β

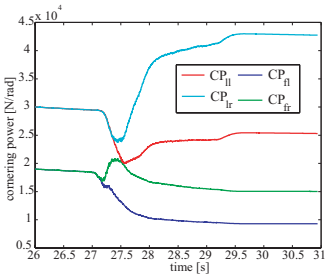

(b)identified value of cornering power

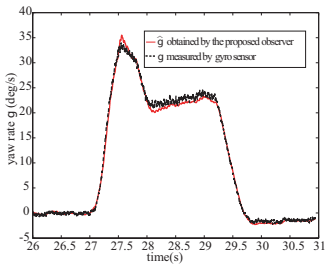

(c)measured value and observer's output of γ

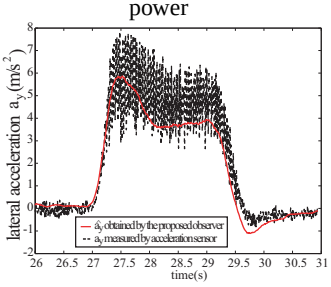

(d)measured value and observer's output of a_y

Fig. 7. estimation results; steering angle δ is 90[deg]

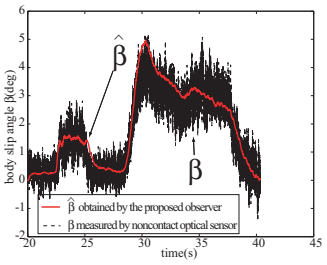

(a)measured value and estimation of β

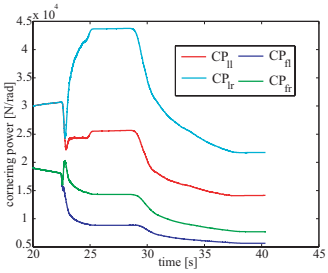

(b)identified value of cornering power

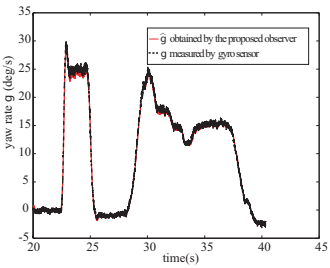

(c)measured value and observer's output of γ

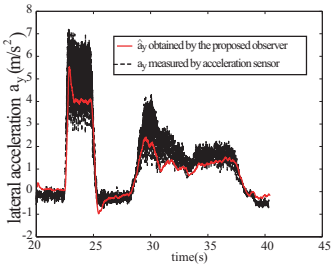

(d)measured value and observer's output of a_y

Fig. 8. estimation results; steering angle δ is 180[deg]

Fig. 8 is experimental results in nonlinear region. Because δ is larger than δ in Fig. 7, β becomes larger and EV enters non-linear region. Fig. 8 demonstrates that the novel observer can estimate β even in non-linear region. In Fig. 8 (b), estimated Conering powers is smaller than in linear region.

VIII. Design of β controller

Body slip angle β must be controlled for driver's safety. We proposed this method based on DYC (Direct Yaw Moment control), which makes full use of EVs' advantages.

Proposed method is based on PID controller and MFC (Model Following Control).

We did experiments by UOT March II to demonstrate the effectiveness of our control method.

A. Model Following Control (MFC)

We utilize Model Following Control (MFC) in order to generate the reference of the vehicle dynamics, or the "desired" response to driver's input [2]. In this paper, MFC calculates the desired value β_{ref}.

We use linear state equations expressed by Equ. (1) as the desired model. Using Equ. (1), β_{ref} is:

$$\beta_{ref} = \frac{(s-a_{22})b_{11}+a_{12}b_{21}}{(s-a_{11})(s-a_{22})-a_{12}a_{21}}\delta_f \tag{28}$$

where matrix A and B are defined in Equ. (1)

If we can keep β following the desired value β_{ref} freely, EVs' movements and safety will be improved dramatically.

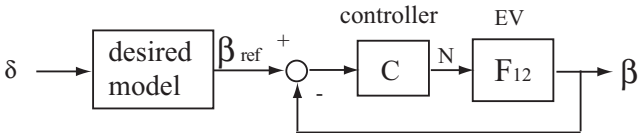

Fig. 9. the proposed control diagram

B. Design of body slip controller

The proposed control diagram is Fig. 9. We control body slip angle β by yaw rate N. We use linear two wheel (Equ. 1)model for PID controller to make EV's advantage, that is "motor's torque generation is fast and accurate".

F_{12} is transfer function from input yaw moment N to body slip angle β.

$$F_{12} = \frac{a_{12}b_{22}}{(s-a_{11})(s-a_{22})-a_{12}a_{21}} \tag{29}$$

Transfer function from β_{ref} to β in Fig. 9 is:

$$\frac{\beta}{\beta_{ref}} = \frac{CF_{12}}{1+CF_{12}} \tag{30}$$

To decide poles of the transfer function in Equ. (30) freely, we use PID gain (Equ. (31)).

$$C = K_1 s + K_2 + \frac{K_3}{s} \tag{31}$$

By Equs. (29), (31) and (30), we can get following equation.

$$\frac{\beta}{\beta_{ref}} = \frac{(K_1s^2+K_2s+K_3)a_{12}b_{22}}{s^3-s^2(a_{11}a_{22}-a_{12}a_{21})+(K_1s^2+K_2s+K_3)a_{12}b_{22}} \tag{32}$$

This denominator of Equ. (32) is:

$$\begin{aligned} denominator = s^3 + s^2(-a_{11} - a_{22} + K_1 a_{12} b_{22}) \\ + s(a_{11}a_{22} - a_{12}a_{21} + K_2 a_{12} b_{22}) \\ + K_3 a_{12} b_{22} \end{aligned} \quad (33)$$

By pole placement method, we design this denominator as:

$$denominator = (s-\alpha)(s-\beta)(s-\gamma) \quad (34)$$

α, β and γ are poles of Equ. (30)

By Equs. (33) and (34), PID gains are expressed in Equ. (37).

$$\begin{aligned} \alpha\beta\gamma &= -K_3 a_{12} b_{22} \\ \alpha\beta + \beta\gamma + \gamma\alpha &= a_{11}a_{22} - a_{12}a_{21} + K_2 a_{12} b_{22} \\ \alpha + \beta + \gamma &= -(-a_{11} - a_{22} + K_1 a_{12} b_{22}) \end{aligned} \quad (35)$$

$$\Updownarrow$$

$$\begin{aligned} K_1 &= \frac{a_{11} + a_{22} - (\alpha + \beta + \gamma)}{a_{12} b_{22}} \\ K_2 &= \frac{\alpha\beta + \beta\gamma + \gamma\alpha - a_{11}a_{22} + a_{12}a_{21}}{a_{12} b_{22}} \\ K_3 &= -\frac{\alpha\beta\gamma}{a_{12} b_{22}} \end{aligned} \quad (36)$$

IX. Experimental demonstration for control and estimation by UOT MarchII

A. Experiment setup for the proposed control

We did some experiments by UOT MarchII to verify the effectiveness of proposed controller and the proposed observer under the novel control. One of the experimental results was shown.

B. Estimation and contorl results

Experiments' results by UOT MarchII are shown as Figs. 10.

Fig. 10 is experimental results in linear region. Speed is 40km/h and driver's input steering wheel angle δ is 150[deg]. Fig. 10 (a-1) is estimation and measured body slip angle β with control and without control to verify the proposed control.

Fig. 10 (a-2) is identified cornering power with the proposed method.

Fig. 10 (b) and (c) are measured and output a_y and γ.

Fig. 10 (a-1) shows us that body slip angle β is suppressed by the proposed control. This figure demonstrates the effectiveness of the novel control. Moreover, estimated β coresponds with measured β. This figure demonstrates that the novel proposed observer can estimate β in linear region even if β is controlled by yaw moment N.

X. Conclusion

In this paper, we proposed novel methods to estimate β, to identify cornering power and to control β for EVs. The improved observer is based on acceleration and yaw rate γ sensors. By this method, we can estimate β robustly and accurately. The results of experiments by using UOT March II demonstrated that the proposed observer could estimate β exactly and robustly.

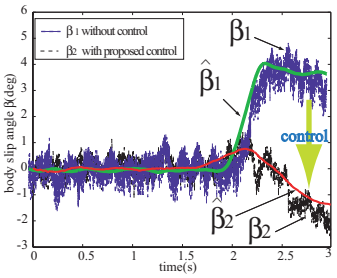

(a-1)Comparison β with normal and the proposed control

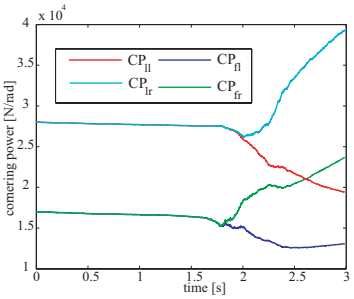

(a-2)identified cornering power

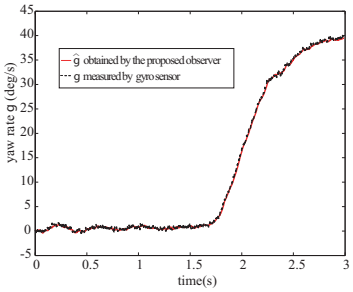

(b)measured value and observer's output of γ

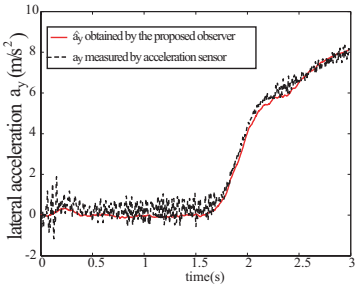

(c)measured value and observer's output of a_y

Fig. 10. β control and estimation results

Next, We utilize MFC and PID controller for EVs' motion control by yaw moment N. Experimental results by by UOT March II demonstrate the effectiveness of the proposed method and show us that the proposed linear observer can estimate β under the novel control in any region.

References

[1] Yoichi Hori: "Future Vehicle driven by Electricity and Control -Research on 4 Wheel Motored 'UOT March II'", AMC 2002, pp.1-14, 2002.

[2] Shinichiro Sakai, Hideo Sado and Yoichi Hori: "Motion Control in an Electric Vehicle with Four Independently Driven In-Wheel Motors", $IEEETrans.onMechatronics$, Vol.4, No.1, pp.9-16, 1999.

[3] Masugi Kaminaga and Genpei Naito: "Vehicles Body Slip Angle Estimation Using an Adaptive Observer", $Proceedings\ of\ AVEC'98$, 1998.

[4] Aleksander D.Rodic and Minmir K. Vukobratovic: "Contribution to the Integrated Control Synthesis of Road Vehicles", $IEEE\ Transactions\ on\ Control\ Systems\ Technology$, Vol.7, No.1, 1999.

[5] Laura R. Ray: "Nonlinear Tire Force Estimation and Road Friction Identification Simulation and Experiments" $Automatica$, Vol.33, No.10,pp.1819-1833,1997.

[6] Laura R. Ray: "Nonlinear State and Tire Force Estimation for Advanced Vehicle Control", $IEEE\ Transactions\ on\ Control\ Systems\ Technology$, Vol.3, No.1, pp.117-124, 1995.

[7] Fredrik Gustafsson: "Monitoring Tire-Road Friction Using The Wheel Slip", $IEEE\ Control\ Systems$, pp.42-49, 1998.

[8] Tomoko Inoue and Yoichi Hori: "Observer Design of Body Angle β for Future Vehicle Control and Experimental Evaluation using the Four-Motored Electric Vehicles", $EVS-20$, 2003.

[9] Yoichi Hori and Takaji Umeno: Implementation of Robust Flux Observer Based Field Orientation (FOFO) Controller for Induction Machines" 1989 $IASAnnual\ Meeting$, pp.523-528, 1989.